

# Articles

## Solution Conformations of Patellamides B and C, Cytotoxic Cyclic Hexapeptides from Marine Tunicate, Determined by NMR Spectroscopy and Molecular Dynamics

Toshimasa Ishida,\* Yasuko In, Fumiyo Shinozaki, and Mitsunobu Doi

Osaka University of Pharmaceutical Sciences, 2-10-65 Kawai, Matsubara, Osaka 580, Japan

Daisuke Yamamoto

Biomedical Computation Center, Osaka Medical College, 2-7 Daigaku-machi, Takatsuki 569, Japan

Yasumasa Hamada and Takayuki Shioiri

Faculty of Pharmaceutical Sciences, Nagoya City University, Tanabe-dori, Mizuho-ku, Nagoya 467, Japan

Miyoko Kamiguchi\* and Makiko Sugiura

Kobe Pharmaceutical University, 4-19-1 Motoyamakita-machi, Higashinada-ku, Kobe 658, Japan

Received December 5, 1994 (Revised Manuscript Received April 14, 1995<sup>o</sup>)

In order to elucidate a possible relationship between the chemical structure and molecular conformation/stability of cytotoxic cyclic hexapeptides from a marine tunicate, *Lissoclinum patella*, the solution conformations of patellamides B and C, the chemical structures of which deviate from the  $C_2$ -symmetry at two positions, were analyzed by means of  $^1\text{H-NMR}$  spectroscopy and restrained molecular dynamics simulation. The two molecules took similar twisted "figure eight-like" backbone conformations without intramolecular hydrogen bonding (type III) in chloroform solution. The outline of these cyclic backbone conformations is similar to that of a related non- $C_2$ -symmetric patellamide D observed in the crystal structure, but deviates significantly from the "square form" (type I) of the  $C_2$ -symmetric ascidiacyclamide or the slightly structurally deformed patellamide A. Results indicate that preference for the type I or III conformation is dependent on the degree of asymmetry of the side chains attached to the two halves of the  $C_2$ -symmetric backbone structure. The possible conformation of the cytotoxic cyclic hexapeptide is discussed in relation to its biological activity.

### Introduction

Interest in marine organisms has been steadily increasing, primarily due to the presence of metabolites capable of acting as potent cytotoxic, antineoplastic, or antiviral agents.<sup>1</sup> The marine tunicate (ascidian) *Lissoclinum patella* produces a series of antineoplastic cyclic hexapeptides (Figure 1), all of which contain unusual thiazole and oxazoline amino acids.<sup>2</sup> As part of a program to elucidate the stereostructure–activity relationship of these cytotoxic cyclic hexapeptides, we analyzed the conformations of ascidiacyclamide, patellamide A and ulithiacyclamide by X-ray crystallography,  $^1\text{H-NMR}$  spectroscopy, or molecular dynamics (MD) simulations.<sup>3</sup> All of the cyclic hexapeptides analyzed so far showed a  $C_2$ - or pseudo- $C_2$ -symmetric square form of type I (Figure 2). Since this conformation is also the predomi-

nant form of ulithiacyclamide (the most cytotoxic peptide in Figure 1) in solution,<sup>3b</sup> the relationship of the type I square form conformation with the biological activity has been considered.

On the other hand, it was reported by Schmitz *et al.*<sup>4</sup> that the crystal structure of patellamide D, the only example so far analyzed of the cyclic hexapeptides having non- $C_2$ -symmetric side chains, takes a type IV conformation stabilized by four intramolecular hydrogen bonds. Since the type IV conformation could be converted to type I *via* types II and III, it appears important, in the consideration of the "active" conformation of these cyclic hexapeptides, to know the factors which dominate the preference for either type I or IV conformation. From the comparison of the chemical structures of ascidiacy-

<sup>o</sup> Abstract published in *Advance ACS Abstracts*, June 1, 1995.

(1) (a) Davidson, B. S. *Chem. Rev.* **1993**, *93*, 1771–1791. (b) Fusetani, N.; Matsunaga, S. *Chem. Rev.* **1993**, *93*, 1793–1806. (c) Michael, J. P.; Pattenden, G. *Angew. Chem., Int. Ed. Engl.* **1993**, *32*, 1–23. (d) Faulkner, D. J. *Nat. Prod. Rep.* **1992**, *9*, 323–364; **1991**, *8*, 97–147; **1990**, *7*, 269–309.

(2) (a) Ireland, C. M.; Durso, A. R., Jr.; Newman, R. A.; Hacker, M. P. *J. Org. Chem.* **1982**, *47*, 1807–1811. (b) Hamamoto, Y.; Endo, E.; Nakagawa, M.; Nakanishi, T.; Mizukawa, K. *J. Chem. Soc., Chem. Commun.* **1983**, 323–324.

(3) (a) Ishida, T.; Tanaka, M.; Nabae, M.; Inoue, M.; Kato, S.; Hamada, Y.; Shioiri, T. *J. Org. Chem.* **1988**, *53*, 107–112. (b) Ishida, T.; Ohishi, H.; Inoue, M.; Kamiguchi, M.; Sugiura, M.; Takao, N.; Kato, S.; Hamada, Y.; Shioiri, T. *J. Org. Chem.* **1989**, *54*, 5337–5343. (c) Ishida, T.; In, Y.; Doi, M.; Inoue, M.; Hamada, Y.; Shioiri, T. *Biopolymers*, **1992**, *32*, 131–143. (d) In, Y.; Doi, M.; Inoue, M.; Ishida, T.; Hamada, Y.; Shioiri, T. *Chem. Pharm. Bull.* **1993**, *41*, 1686–1690. (e) In, Y.; Doi, M.; Inoue, M.; Ishida, T.; Hamada, Y.; Shioiri, T. *Acta Crystallogr.* **1994**, *C50*, 432–434. (f) In, Y.; Doi, M.; Inoue, M.; Ishida, T.; Hamada, Y.; Shioiri, T. *Acta Crystallogr.* **1994**, *C50*, 2015–2017.

(4) Schmitz, F. J.; Ksebaty, M. B.; Chang, J. S.; Wang, J. L.; Hossain, M. B.; van der Helm, D.; Engel, M. H.; Serban, A.; Silfer, J. A. *J. Org. Chem.* **1989**, *54*, 3463–3472.

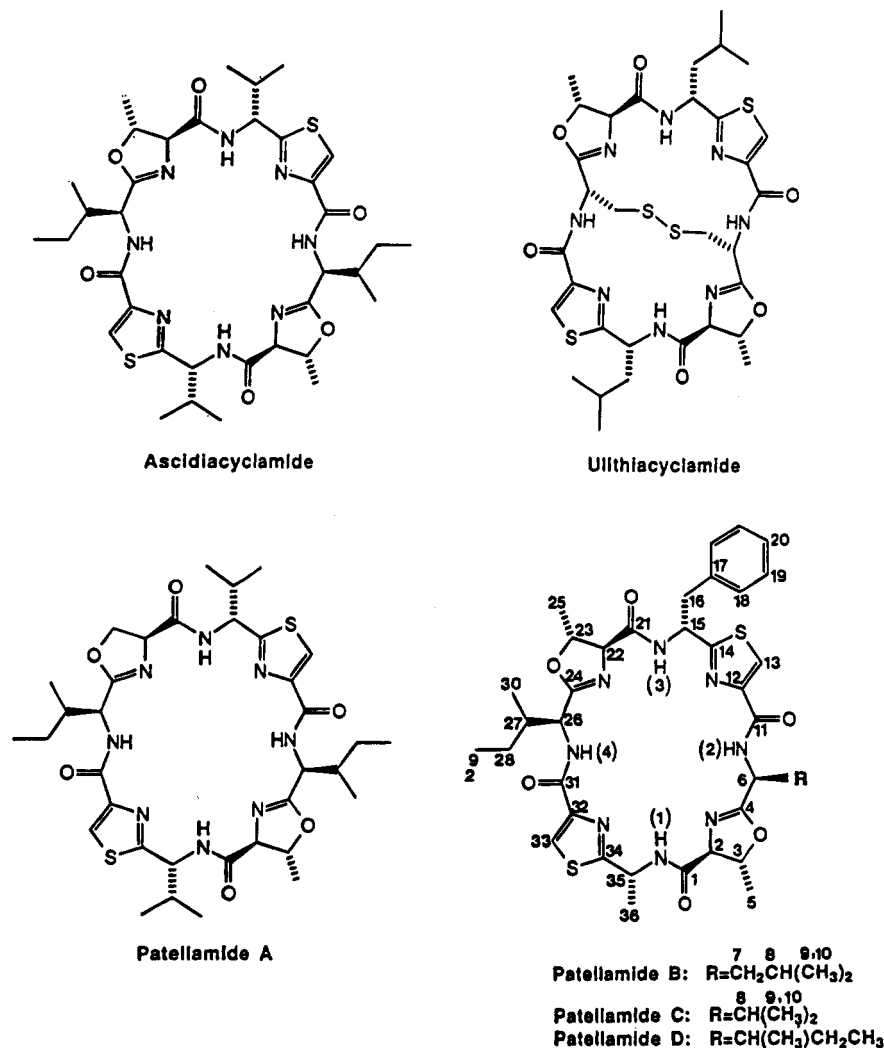


**Figure 1.** Chemical structures of several cytotoxic cyclic peptides isolated from the tunicate *Lissoclinium patella*. Numbering of atomic positions for patellamides B and C is also given.

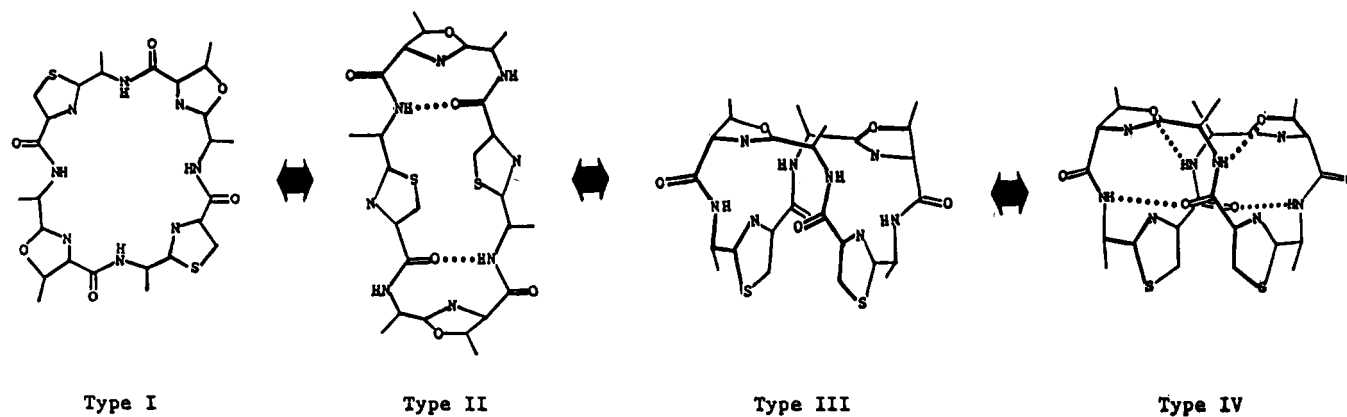


**Figure 2.** Schematic illustrations of possible conformational transitions among types I, II, III, and IV. The "type IV-like" conformation without intramolecular hydrogen bonding is newly classified as type III.

clamide and patellamide D (Figure 1), it appears that the deviation from the  $C_2$ -symmetric chemical structure triggers the shift of the molecular conformation from type I type IV. In this context, the present paper deals with the molecular conformations of patellamides B and C, determined by a combination of NMR spectroscopy in chloroform solution and the restrained MD simulations; non- $C_2$ -symmetry was observed between the D-Phe-D-Ala and Ile-Leu positions for patellamide B and between the D-Phe-D-Ala and Ile-Val for patellamide

C (Figure 1). These results would provide useful information on the chemical structure-molecular conformation relationship of these compounds.

### Results

**NMR Assignments.** Numbering of atomic positions in this work is shown in Figure 1. Assignments of  $^1\text{H}$ - and  $^{13}\text{C}$ -NMR peaks were mainly based on connectivity information from homo- and heteronuclear scalar couplings. Assignment of the  $^1\text{H}$  peaks for patellamides B

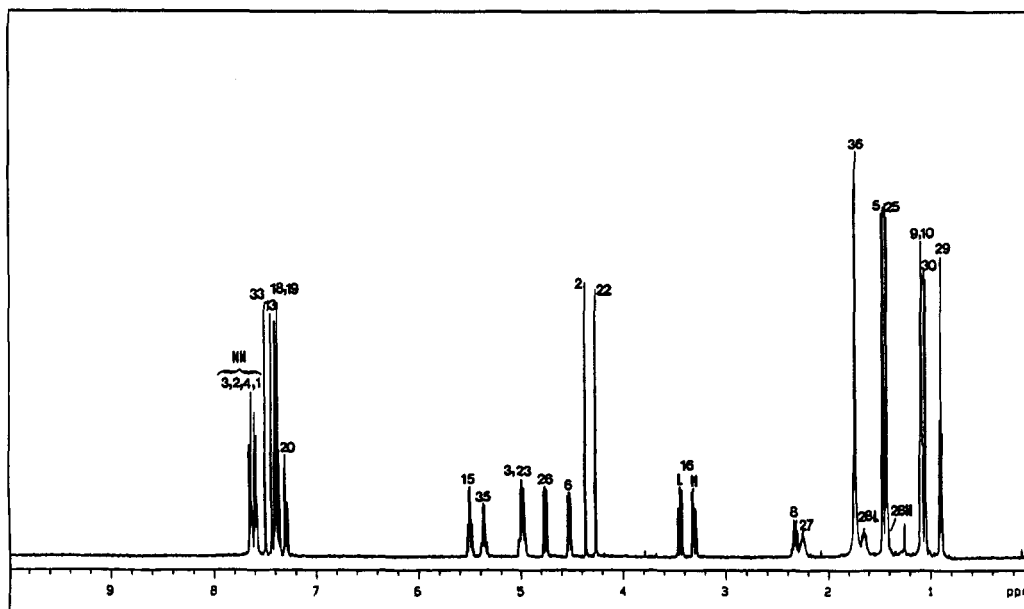


**Figure 3.** The 500-MHz  $^1\text{H}$ -NMR spectrum of patellamide C in  $\text{CDCl}_3$  solution at 24  $^\circ\text{C}$ . Numbers correspond to those in Figure 1. Diastereotopic protons of high- and low-field sides are represented as (H) and (L), respectively. Nearly the same spectrum is also obtained for patellamide B.

and C in  $\text{CDCl}_3$  solution was made using a combination of TOCSY (total correlation spectroscopy) and COSY (correlated spectroscopy) experiments. Sequential assignment was achieved from the analysis of NOESY (nuclear Overhauser enhancement spectroscopy) spectra and the homoallylic couplings between H2 and H6 protons and between H22 and H26 protons, where the D-Phe aromatic protons were chosen as a starting point for assignment. The 1D proton peaks of patellamide C are shown in Figure 3; the proton peaks of patellamide B were assigned in the same manner. In contrast to that of  $C_2$ -symmetric ascidiacyclamide or ulithiacyclamide, the  $^1\text{H}$  NMR spectrum of patellamide B or C revealed about twice the number of peaks due to the deviation from the  $C_2$ -symmetric chemical structure. On the other hand, assignment of  $^{13}\text{C}$  peaks was carried out through a combination of DEPT (distortionless enhancement by polarization transfer),  $^{13}\text{C}$ - $^1\text{H}$  shift correlation, and HMQC (heteronuclear multiple-quantum coherence) and HMBC (heteronuclear multiple-bond coherence) measurements; these measurements gave additional verification of the  $^1\text{H}$  assignment. The selective inverse  $^{13}\text{C}$ - $^1\text{H}$  long-range correlations<sup>5</sup> of HMBC spectra enabled the distinctions between C13 and C33, between C2 and C22, and between C3 and C23 atoms, as well as the diastereotopic assignment of  $\text{CH}_2$  protons [C7, C16, and C28 atoms for patellamide B and C16 and C28 atoms for patellamide C].  $^1\text{H}$ -, and  $^{13}\text{C}$ -NMR data for patellamides B and C are summarized in Tables 1 and 2, respectively. Although peak assignments of  $^1\text{H}$  resonances of patellamide B were almost the same as those in  $\text{DMSO}-d_6$  by Sesin *et al.*,<sup>6</sup> significant differences were observed in H8 and NH1-NH4 proton chemical shifts. Similarly, notable differences were observed in the assignment of  $^{13}\text{C}$  resonances of C5, C9, and C10 atoms. These differences could be accounted for by the difference in solvent used, although the chemical shift (= 2.08 ppm) of H8 reported by Sesin *et al.* could be assigned to one of two H7 protons.

**Table 1.**  $^1\text{H}$ -NMR Data for Patellamides B and C<sup>a</sup>

H at C no.	patellamide B	patellamide C
2	4.358 (d, 2.7) <sup>b</sup>	4.355 (d, 2.5)
3	4.985 (m)	4.999 (m)
5	1.433 (d, 5.0)	1.462 (d, 6.5)
6	5.00 (m)	4.524 (dd, 7.5, 11.2)
7H <sup>c</sup>	1.575 (m)	
7L <sup>c</sup>	2.133 (m)	
8	1.64 (m)	2.321 (m)
9	1.008 (d, 6.5)	1.084 (d, 6.5)
10	1.046 (d, 6.7)	1.090 (d, 6.4)
13	7.402 (s)	7.431 (s)
15	5.482 (ddd, 5.9, 9.9, 10.5)	5.496 (ddd, 5.5, 9.9, 10.2)
16H <sup>c</sup>	3.298 (dd, 5.9, 14.5)	3.307 (dd, 5.5, 13.8)
16L <sup>c</sup>	3.435 (dd, 10.5, 14.5)	3.436 (dd, 10.2, 13.8)
18	7.402	7.397
19	7.367	7.363
20	7.290	7.287
22	4.263 (d, 2.8)	4.258 (d, 2.5)
23	4.985 (m)	4.970 (m)
25	1.447 (d, 5.0)	1.425 (d, 6.5)
26	4.747 (dd, 7.5, 11.5)	4.760 (dd, 7.5, 11.3)
27	2.262 (m)	2.245 (m)
28H <sup>c</sup>	1.43 (m)	1.43 (m)
28L <sup>c</sup>	1.663 (m)	1.65 (m)
29	0.909 (t, 7.2)	0.898 (t, 7.5)
30	1.062 (d, 6.7)	1.049 (d, 6.3)
33	7.467 (s)	7.495 (s)
35	5.363 (dq, 9.9, 6.9)	5.363 (dq, 10.0, 7.0)
36	1.732 (d, 6.9)	1.734 (d, 7.0)
NH1	7.615 (d, 9.9)	7.585 (d, 10.0)
NH2	7.633 (d, 7.5)	7.633 (d, 7.5)
NH3	7.609 (d, 9.9)	7.635 (d, 9.9)
NH4	7.577 (d, 7.5)	7.587 (d, 7.5)

<sup>a</sup> 500 MHz. <sup>b</sup> Chemical shift ( $\delta$ ) (mult,  $J$  in Hz). <sup>c</sup> Diastereotopic protons of high-field side (H) and low-field side (L).

**Vicinal Coupling Constants and Temperature Dependence of NH Protons.** To obtain information on the conformation around N-C $\alpha$  and C $\alpha$ -C $\beta$  bonds, vicinal proton coupling constants ( $^3J_{\text{NHC}\alpha\text{H}}$  and  $J_{\text{HC}\alpha\text{C}\beta\text{H}}$ ) were determined from  $^1\text{H}$ -NMR spectral data (Table 1), and possible torsion angles were estimated using a Karplus-type equation.<sup>7</sup> The results are given in Table 3, where torsion angles of the most stable structure

(5) Agrawal, P. K. *Phytochemistry* **1992**, *31*, 3307-3330.

(6) Sesin, D. F.; Gagkell, S. J.; Ireland, C. M. *Bull. Soc. Chim. Belg.* **1986**, *95*, 853-867.

Table 2.  $^{13}\text{C}$ -NMR Data for Patellamides B and C<sup>a</sup>

C no.	patellamide B	patellamide C
1	173.121	173.149
2	73.828	73.743 <sup>c</sup>
3	82.508	82.543 <sup>d</sup>
4	168.398	168.103
5	20.995	21.136
6	47.759	55.983
7	38.945	
8	25.044	27.949
9	21.795 <sup>b</sup>	19.346 <sup>e</sup>
10	23.206 <sup>b</sup>	19.760 <sup>e</sup>
11	161.669	161.914
12	147.197	147.396
13	123.713	123.818
14	170.812	170.910
15	52.460	52.404
16	40.742	40.875
17	136.330	136.330
18	129.305	129.305
19	128.786	128.772
20	127.186	127.172
21	173.465	173.324
22	73.786	73.722 <sup>c</sup>
23	82.115	82.501 <sup>d</sup>
24	168.124	168.223
25	20.995	20.813
26	53.260	53.267
27	32.904	32.805
28	25.030	24.981
29	8.771	8.722
30	14.996	15.157
31	161.900	161.935
32	147.690	147.697
33	123.579	123.713
34	172.819	172.756
35	46.657	46.678
36	20.778	21.157

<sup>a</sup> 125.7 MHz. <sup>b,c,d,e</sup> Interchangeable.

Table 3. Possible Torsion Angles from  $3J_{\text{NHCOH}}$  and  $J_{\text{HC}\alpha\beta\text{H}}$  Coupling Constants and from MD Calculations, Together with Temperature Coefficients of NH Protons

bond sequence		torsion angle (NMR)		torsion angle (MD)	
		pate B <sup>a</sup>	pate C	pate B	pate C
C1-N1-C35-C34/	$\phi^b$	102°, -222°	102°, -222°	81°	81°
C21-N3-C15-C14				84°	98°
C11-N2-C6-C4/	$\phi$	-85°, 205°	-85°, 205°	-75°	-74°
C31-N4-C26-C24				-87°	-76°
H-C6-C7-H	$\theta^c$			178°, 64°	
H-C6-C8-H	$\theta$		160°		177°
H-C15-C16-H(H) <sup>d</sup>	$\theta$	41°, 127°	44°, 125°	58°	61°
H-C15-C16-H(L)	$\theta$	152°	152°	175°	178°
H-C26-C27-H	$\theta$	163°, -103°	163°, -103°	182°	181°

$\Delta\delta/dT \times 10^4$ , ppm/°C

NH	$\Delta\delta/dT \times 10^4$ , ppm/°C	
	pate B	pate C
NH1	10.0	11.3
NH2	11.5	9.3
NH3	8.0	9.5
NH4	9.3	6.3

<sup>a</sup> Patellamides B and C are abbreviated as pate B and pate C, respectively. <sup>b</sup>  $3J_{\text{HNCOH}} = 9.8 \cos^2 \theta - 1.1 \cos \theta + 0.4 \sin^2 \theta$ , where  $\phi = |\theta - 60|^\circ$  for L-isomer and  $\phi = |\theta + 60|^\circ$  for D-isomer. Among four values obtained from the equation, only possible angles are given based on the model consideration. <sup>c</sup>  $J_{\text{HC}\alpha\beta\text{H}} = 11.0 \cos^2 \theta - 1.4 \cos \theta + 1.6 \sin^2 \theta$ . Only two possible are given. <sup>d</sup> Diastereotopic protons of high-field and low-field sides are represented as (H) and (L), respectively.

derived from MD simulations (to be discussed later) are also given for comparison. On the other hand, the

Table 4. Averaged  $r_{ij}$  Values Estimated for Several Protons Pairs from Relaxation Method and from MD Calculations

Hi	Hj	$r_{ij}$ (Å) from NMR	$r_{ij}$ (Å) from MD	Hi	Hj	$r_{ij}$ (Å) from NMR	$r_{ij}$ (Å) from MD
Patellamide B							
NH1	13	3.4	4.1	NH1	35	3.4	2.9
NH1	36	2.9	2.5	NH2	6	2.4	2.9
NH2	7L	2.6	2.4	NH2	7H	3.1	3.5
NH2	23	2.5	3.5	NH2	27	3.4	3.5
NH3	15	3.8	2.9	NH3	16L	2.7	2.5
NH3	16H	3.7	3.5	NH4	3	2.8	3.5
NH4	7L	3.6	3.5	NH4	7H	3.3	3.1
NH4	26	2.7	2.9	NH4	27	2.5	2.5
NH4	28	2.8	2.3	2	3	3.3	2.9
6	7L	3.3	2.5	13	36	4.5	4.1
15	16L	3.1	3.5	15	16H	2.7	2.5
16L	33	3.3	2.8	22	23	3.1	2.9
26	27	2.8	3.3				
Patellamide C							
NH1	2	3.1	3.5	NH1	13	3.8	4.1
NH1	35	3.1	2.9	NH1	36	2.8	2.5
NH2	6	3.2	2.9	NH2	8	2.5	2.4
NH2	13	4.8	4.5	NH2	23	2.7	3.1
NH2	27	4.0	3.5	NH3	15	3.2	3.0
NH3	16L	2.7	2.5	NH3	16H	3.6	3.5
NH3	22	3.3	3.4	NH3	33	3.1	4.1
NH4	3	2.9	3.4	NH4	8	3.1	3.5
NH4	26	3.4	2.9	NH4	27	2.6	2.5
2	3	3.0	2.9	6	8	3.9	3.1
13	36	4.1	4.1	15	16L	4.0	3.9
15	16H	3.1	3.1	16L	33	3.3	2.9
16H	33	4.1	4.5	22	23	3.1	2.9
26	27	3.9	3.1	35	36	2.8	3.2

temperature dependence of NH protons was measured in the range of 10–50 °C at intervals of 5 °C in order to estimate the possibility of hydrogen bonds in which the NH protons participate. The temperature coefficients, obtained from the least-squares plots, are also given in Table 3. These values were too far from zero to suggest the hydrogen bondings of NH protons. Therefore, it could be concluded that there are no intramolecular hydrogen bonds and that the NH protons are all exposed to chloroform solvent. A similar temperature dependence was shown for patellamide D NH protons, although a detailed measurement was not done because of the deficient amount of sample.

#### Conformationally Relevant NMR Parameters.

The estimation of interproton distances was carried out by a selective relaxation method in which  $r_{ij}$  (distance between protons  $i$  and  $j$ ) can be estimated from a combination of (a) correlation time ( $\tau_c$ ) for molecular reorientation evaluated from the frequency dependence of nonselective  $T_1$  ( $T_1^{\text{NS}}$ ) and (b) cross-relaxations ( $\sigma_{ij}$ ) derived from  $^1\text{H}$  selective and biselective relaxation times ( $T_1^{\text{S}}$  and  $T_1^{\text{BS}}$ ).<sup>8</sup> According to an application of this method to the conformational analyses of organic compounds,<sup>8c</sup> three types of spin–lattice relaxation times were measured, and the  $r_{ij}$  values for some selected proton pairs were evaluated from respective  $\tau_c$  and  $\sigma_{ij}$  values. The results are given in Table 4, where the  $r_{ij}$  values from MD simulations are also given for comparison. Both patellamides B and C take the type III conformation (Figure 2) without any intramolecular hydrogen bonding in solution, judging from the short distances between the NH1–H13, NH2–H23, NH2–H27, NH4–H7L, NH4–H7H, NH4–H3, and H16L–H33

(7) (a) Bystrov, V. F.; Ivanov, V. T.; Portnova, S. L.; Balashova, T. A.; Ovchinnikov, Y. A. *Tetrahedron* **1973**, *29*, 873–877. (b) Kopple, K. D.; Wiley, G. R.; Tauke, R. *Biopolymers* **1973**, *12*, 627–636.

(8) (a) Sugiura, M.; Takao, N.; Fujiwara, H. *Magn. Reson. Chem.* **1988**, *26*, 1051–1057. (b) Sugiura, M.; Sai, T.; Ichimaru, M.; Kato, A.; Takao, N. *Magn. Reson. Chem.* **1991**, *29*, 755–758. (c) Sai, T.; Takao, N.; Sugiura, M. *Magn. Reson. Chem.* **1992**, *30*, 1041–1046.

pairs for patellamide B and the NH1–H13, NH2–H23, NH2–H27, NH3–H33, NH4–H3, NH4–H8, H13–H36, and H16L–H33 pairs for patellamide C and from the large temperature dependence of NH protons. These results were also supported by NOE measurements. Two independent NOESY experiments on patellamides B and C were performed with mixing times of 300 ms at 300 MHz and 400 ms at 500 MHz. In addition to the usual intraresidual NOE peaks, several interresidual NOE cross peaks were observed in both spectra, although the detectable NOEs were not necessarily observed for all short-range proton pairs estimated from the relaxation method (Table 4). Notable NOEs were observed for NH3–H29, H7L–H27, and H16L–H33 proton pairs of patellamide B and for H2–H26, H6–H26, H13–H36, and H16L–H33 proton pairs of patellamide C, suggesting the type III conformation; the NOEs of H16L–H33 [patellamide B] and H13–H36 [patellamide C] pairs are shown in Figure 4.

**Restrained Molecular Dynamics Simulations.** In order to simulate the molecular conformation of patellamide B or C in chloroform solution, the restrained MD simulation was performed with the CHARMM program<sup>9</sup> using the molecular graphics QUANTA (Molecular Simulation Inc., Waltham, MA) parameter set. The initial structure of patellamide B or C was generated using the MMS program (CHEMLAB-II),<sup>10</sup> in which the solid-state conformation<sup>3e</sup> (type I in Figure 2) of patellamide A served as the initial structure for patellamide B or C. The side chains of Phe, Ile, Leu, and Val were fitted to the conformations calculated from the  $J_{\text{HCAcBH}}$  values (Table 3). A harmonic potential was employed for the interproton distances estimated from the relaxation method (Table 4). Error from  $-0.5$  to  $1$  Å was allowed for any distance constraint, under the condition that their lower limits were commonly set to  $1.8$  Å. The torsion angles (Table 3) were not included in the MD calculations as potential restraints; however, they were used as an index for estimating the reliability of the tertiary structure constructed. Dynamic simulation was carried out for 10 ps at 300 K, starting from a constraint-free energy-minimized conformation. Because of cyclization of the backbone structure, the satisfactorily simulated conformers showed nearly the same backbone folding, although a slight variation was observed for each side chain conformation. The most stable conformer is shown in Figure 5 as representative solution conformation of patellamide B or C.

**Energy Minimization of Types I–IV Conformations.** In order to compare the energy stability among type I–IV conformers (Figure 2) of patellamide B or C, energy-minimization calculations were performed using the CHARMM program and the molecular graphics QUANTA parameter set, and results are given in Table 5.

**MD Simulations in Aqueous Solution.** Each imaginary system of patellamides B and C dissolved in water was constructed to simulate the conformational stability of the type I and III conformations under a practical situation, in which 227 (type I) or 202 (type III) water molecules within a sphere of a  $10$  Å radius were placed around the patellamides B and C. To study the type I

conformational stability, the interaction mode with solvent molecules observed in the crystals<sup>3</sup> of ascidiacyclamide (Figure 6) was used. MD simulations were made for 10 ps at 300 K. Nearly the same results were obtained for patellamides B and C.

## Discussion

The schematic illustration of possible conformations of cyclic hexapeptides from an ascidian, together with their possible transition pathways, is shown in Figure 2. The present study was performed to investigate whether the deviation from the  $C_2$ -symmetric chemical structure causes a transition from the type I to the type IV conformation, because the relationship between chemical structure and molecular conformation provides important information for the determination of the "active" conformation and the development of a useful pharmaceutical agent. NMR measurements showed similar conformational behaviors of patellamides B and C, and the estimation of interproton distances from selective and biselective  $T_1$  measurements (Table 4) led to the elucidation of the type III conformation without any intramolecular hydrogen bonding as the major conformer of patellamides B and C in chloroform solution. Moreover, long-range NOEs for some proton pairs provide unequivocal support to the above-mentioned findings.

Taking advantage of the rather limited number of conformations due to the cyclic backbone structure and of the interproton distance information (Table 4), the refinement of the possible conformational structures by restrained MD simulations led to a well-converged type III conformation characterized by the twisted "figure eight-like" structure (Figure 5), where the  $\phi$  torsion angles estimated from the  $^3J_{\text{NHCaH}}$  coupling constants agree well with those of the MD converged structure (Table 3). Irrespective of the difference in amino acid residues (Leu, Ile, and Val), the molecular conformations of patellamides B and C in chloroform solution are essentially the same, and are very similar to the type IV crystal conformation<sup>4</sup> (Figure 5c) of patellamide D in terms of the outline of the peptide backbone structure.

**Type III as the Major Solution Conformation of Non- $C_2$ -Symmetric Cyclic Hexapeptide.** A significant difference could be observed between the conformations of types III and IV. In the type III solution conformations of patellamides B and C, all NH protons do not participate in the formation of intramolecular hydrogen bonds (Figure 5a,b), as is suggested by the high-temperature coefficients of the four NH protons (Table 3). A similar conformation could be also expected for the solution conformation of patellamide D, which is in contrast with its type IV crystal conformation stabilized by four intramolecular hydrogen bonds (Figure 5c). Despite such a difference, the conformations of types III and IV are highly similar. This fact provides an important insight that the formation of intramolecular hydrogen bonds is not necessarily a requisite condition for a twisted "figure eight-like" (type III or IV) structure; although it functions as a stabilizing force, the energy difference between the type III and IV conformations is not as large as expected (Table 5). The type III conformation would mainly be formed by van der Waals interactions between different groups within the non- $C_2$ -symmetric chemical structure, including the  $\pi$ - $\pi$  stacking interaction of thiazole rings. On the basis of results from NMR experiments, generally we can say that the

(9) Brooks, B. R.; Bruccoleri, R. E.; Olafson, B. D.; States, D. J.; Swaminathan, S.; Karplus, M. *J. Comput. Chem.* **1983**, *4*, 187–217.

(10) CHEMLAB-II, a molecular modeling software system; Molecular Design, Ltd.: San Leandro, CA, 1986.

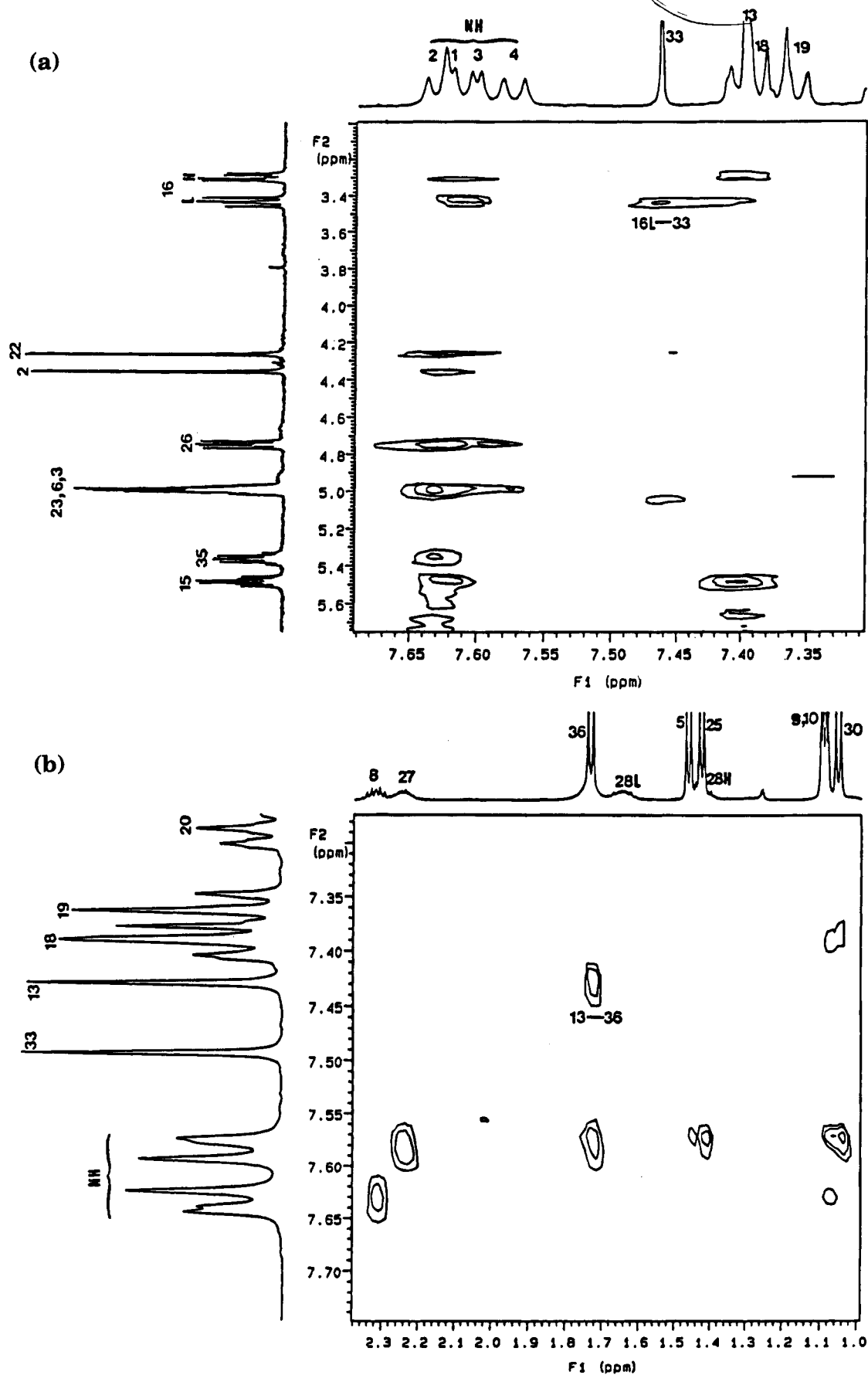


**Figure 4.** Cross peaks of 16L-33 and 13-36 proton pairs in partial NOESY spectra of patellamides B (a) and C (b) in  $\text{CDCl}_3$  solution, respectively.

non- $C_2$ -symmetric cyclic hexapeptide takes the type III conformation preferentially, and the type IV conforma-

tion occurs only in the crystal state or nonpolar solution state, because the interaction of NH protons with organic

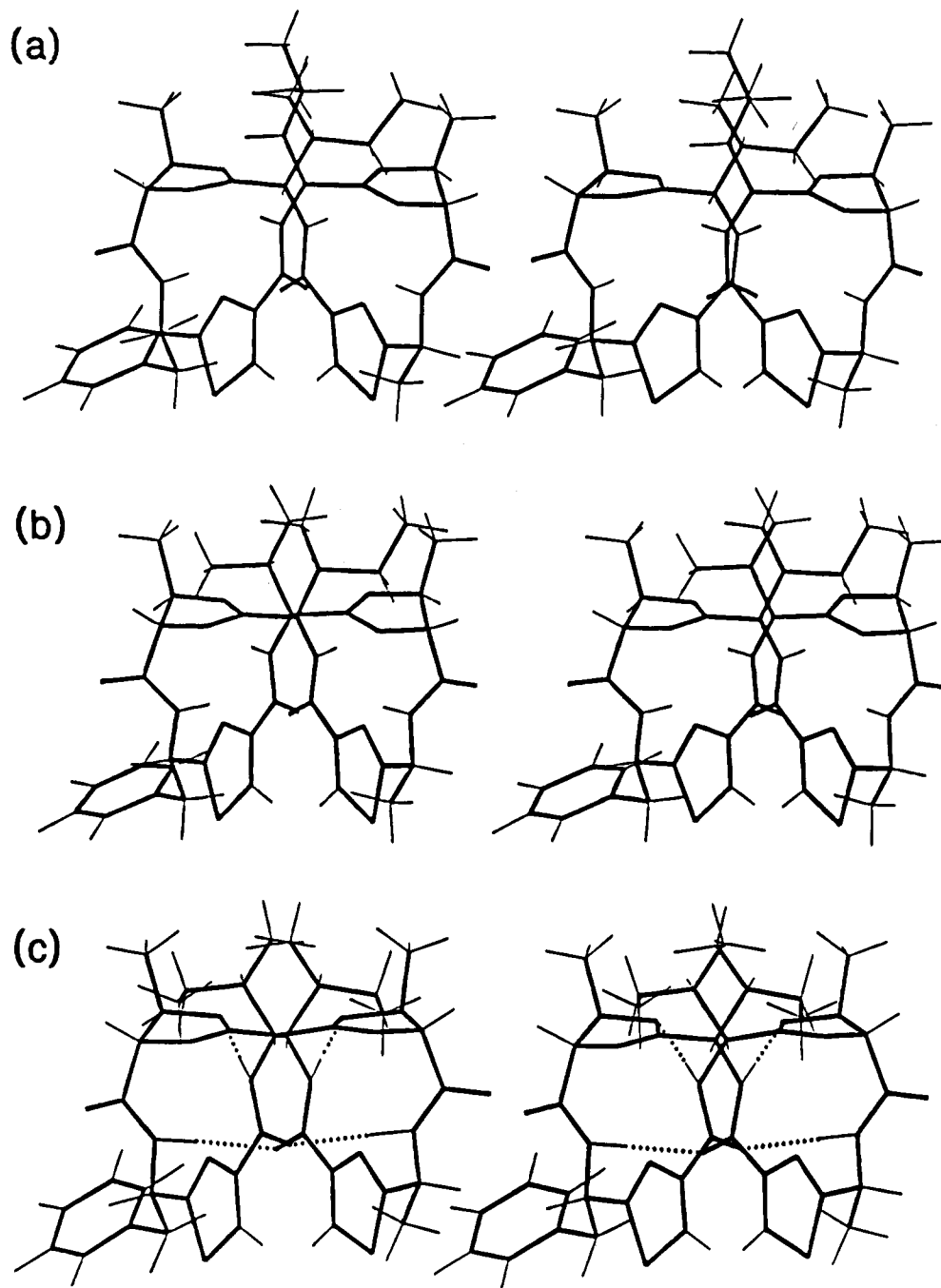


**Figure 5.** Stereoscopic views of the most stable solution conformers of patellamides B (a) and C (b) derived from restrained MD simulations, together with the crystal conformation (type IV) of patellamide D (c) for comparison. The dotted lines represent intramolecular hydrogen bonds.

**Table 5. Total Energies of Different Conformations of Patellamides B and C in Isolated State**

conformation	total energy (kcal/mol)	
	patellamide B	patellamide C
type I	-25.28	-20.03
type II	-36.14	-29.76
type III	-49.74	-42.42
type IV	-50.45	-43.41

solvents would disrupt such intramolecular hydrogen bond formation.

**Conformational Features of Types I and III.** The experimental data obtained so far suggested that the  $C_2$ -symmetric chemical structure of ascidiacyclamide or ulithiacyclamide prefers the type I conformation in the solution and crystal states.<sup>3</sup> In contrast, the present

results indicated the preference for the type III conformation of non- $C_2$ -symmetric patellamide B, C, or D. Thus, the molecular conformations of cyclic hexapeptides isolated from ascidian (Figure 1) are closely related to their chemical structures, and are highly dependent on the degree of asymmetry of the side chains attached to the two halves of the  $C_2$ -symmetric backbone structure. The type I conformation can resist, to a certain extent, the transition to type III caused by partial deformation of the  $C_2$ -symmetric structure, because patellamide A, which exhibits a partial deformation of the  $C_2$ -symmetric chemical structure at the oxazoline methyl group (Figure 1), has also been shown to take a type I conformation<sup>3d,e</sup> in the crystal state. However, it is obvious from the present study that the type III conformation is preferred

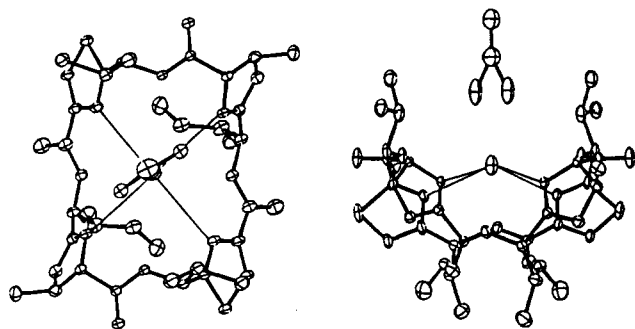


**Figure 6.** Trapping of water and ethanol molecules by the type I conformation of ascidiacyclamide, viewed from the  $C_2$ -symmetry axis (left) and perpendicular to the axis (right). Oxygen atom of water was stably located on the  $C_2$ -symmetry axis by hydrogen bond formation and electrostatic interaction with the thiazole and oxazoline N atoms and peptide NH groups (thin lines). The methyl group of ethanol is disordered into two different positions with respective occupancies = 0.5.

when the extent of asymmetry from the  $C_2$ -symmetric chemical structure exceeds a certain critical level.

On the basis of the above discussion, it would be reasonable to propose that type I and III conformations are the major conformations of the cyclic hexapeptides isolated from ascidian. Aside from the difference of the folding of cyclic backbone structure, one of the most characteristic differences between type I and III conformations is the spatial disposition of the peptide NH groups. The NH groups with the type III conformation could form intramolecular hydrogen bonds with carboxyl or oxazole oxygen atoms without any significant constraint, as is observed in the type IV conformation (Figure 5c). On the other hand, NH groups with the type I conformation could not participate in intramolecular hydrogen bonding, but served as donor/acceptor groups during interaction with the external polar group such as phosphate ions or solvents; for example, the benzene, water or methanol molecule could be trapped in the type I conformation in the case of ascidiacyclamide or patellamide A,<sup>3a,c</sup> in which the solvent molecule is stabilized by hydrogen bonding with the NH groups and/or van der Waals interaction with the hydrophobic side chains of Val residues (Figure 6).

**Biological Implication of Type I and III Conformations.** Concerning the conformational energy stability, the type III conformation is stabler than the type I conformation (Table 5), and this is primarily due to the compactness of the former compared with the latter. This result may reflect the importance of the type III conformation as an "active" conformation of the cytotoxic cyclic hexapeptide. On the other hand, it should be also noted that there is no energy preference between the type I and III conformations in the state coexisting with solvent molecules. In the system of an aqueous solution, MD simulations suggested that these two types of conformations are both stable and show no transition between them; the trajectory of intramolecular S...S distance of patellamide B as a function of MD simulation time showed the fluctuation of 10.3–12.3 Å for the type I conformation and 3.4–5.8 Å for the type III conformation, and similar results were also obtained for patellamide C. This would mean that the type I conformation, as well as type III, could exist stably in living cells.

Since ascidiacyclamide (type I) and patellamides B, C, or D (type III) show similar degrees of cytotoxicity,<sup>2</sup> it is difficult to predict which possesses the "active" conforma-

tion of the cytotoxic cyclic hexapeptide. The cytotoxicity may be due to the combined effects of the molecular conformation and the chemical reactivity of side chains, as has already been stated by Schmitz *et al.*<sup>4</sup> Nevertheless, we propose that the type I conformation is more likely to exert biological activity by reacting with a target molecule, since ulithiacyclamide (the most potent cytotoxic compound among the related peptides<sup>2a</sup>) exhibits only the type I conformation due to a disulfide linkage (Figure 1). Therefore, it may be possible to consider that the biological activity of patellamide B, C, or D is exhibited when it takes the type I conformation, provided that the reversible transition between the types I and III conformations does not require a large driving energy under physiological conditions. The possibility of conformational transition in aqueous solution is currently under investigation.

## Experimental Section

**Materials.** Patellamides B and C were synthesized in the manner of previous reports,<sup>11</sup> and their purities were confirmed from HPLC elution profiles and NMR measurements. All other materials were available commercially (reagent grade) and were used without further purification.

**NMR Spectroscopy.** All <sup>1</sup>H- and <sup>13</sup>C-NMR measurements were performed at 24 °C, except for the temperature dependence experiments. Patellamides B and C (approximately 3 mM) were dissolved in CDCl<sub>3</sub>. The solutions were degassed and sealed under vacuum. Chemical shifts were measured relative to internal TMS at 0.0 ppm; the margins of error were within ±0.001 ppm and ±0.3 Hz for <sup>1</sup>H and ±0.008 ppm for <sup>13</sup>C spectra.

Two-dimensional COSY, NOESY, and TOCSY spectra were acquired in the phase-sensitive mode using the standard pulse schemes. Mixing times for NOESY spectra are 400 ms at 500 MHz and 300 ms at 300 MHz, and that for TOCSY spectra is 80 ms. The time-domain matrix consisted for 128 × 1024 complex data points and was zero-filled to obtain a frequency domain matrix of 1024 × 1024 real data points. The <sup>1</sup>H–<sup>13</sup>C shift correlations were measured by HMQC and HMBC spectroscopies using the standard pulse schemes.

Values of nonselective, selective, and biselective  $T_{1s}$  were measured using the previously reported pulse sequences.<sup>7</sup> The values of correlation time for molecular reorientation ( $\tau_c$ ) were evaluated from  $T_{1NS}$  values of two frequencies ( $\omega_1 = 500$ ,  $\omega_2 = 200$ ) according to eq 1.

$$\frac{T_{1NS}(\omega_1)}{T_{1NS}(\omega_2)} = \frac{(5 + 8\omega_2^2\tau_c^2)(1 + 5\omega_1^2\tau_c^2 + 4\omega_1^4\tau_c^4)}{(5 + 8\omega_1^2\tau_c^2)(1 + 5\omega_2^2\tau_c^2 + 4\omega_2^4\tau_c^4)} \quad (1)$$

The cross-relaxations ( $\sigma_{ij}$ ), obtained from the values of  $T_{1S}$  and  $T_{1BS}$ , and the interproton distances ( $r_{ij}$ ) were obtained from eqs 2 and 3, respectively.

$$1/T_1^{BS} - 1/T_1^S = R^i(ij) - R^i(i) = N_j\sigma_{ij} \quad (2)$$

$$\sigma_{ij} = \frac{1}{10} \gamma^4 h^2 r_{ij}^{-6} \left[ \frac{6\tau_c}{1 + 4\omega^2\tau_c^2} - \tau_c \right] \quad (3)$$

**Restrained Molecular Dynamics.** Three-dimensional structures of patellamides B and C, which satisfy the interproton distances estimated from  $T_1$  measurements, were constructed by restrained MD simulations. In the first step, each initial structure was constructed from the atomic coordinates of the patellamide A crystal structure<sup>9a</sup> using the MMS program.<sup>10</sup> MD calculations were performed with the CHARMM<sup>9</sup> program using the molecular graphics QUANTA

(11) (a) Hamada, Y.; Shibata, M.; Shioiri, T. *Tetrahedron Lett.* **1985**, *26*, 5155–5158. (b) Hamada, Y.; Shibata, M.; Shioiri, T. *Tetrahedron Lett.* **1985**, *26*, 5159–5162.



program and parameter set. All energy terms were calculated. Energy minimizations were performed with a combination of steepest descents and conjugate gradient methods followed by a refinement using the Newton–Raphson method until the energy difference between successive iterations was less than 0.001 kcal/mol. Distance constraints are included in the CHARMM program by adding an extra potential energy term proportional to the square of the difference between the actual and target distances. MD calculations were carried out for 10 ps at 300 K, after 300 steps (1 step = 1 fs) of heating and 300 steps of equilibration. The data were restored every 100

steps. The force cut of nonbonded forces and distance constraints was not applied.

**Supplementary Material Available:** Tables of observed  $T_1^{\text{NS}}$ ,  $T_1^{\text{S}}$ ,  $T_1^{\text{BS}}$ ,  $\tau_c$ ,  $\sigma_{ij}$ , and  $r_{ij}$  values for patellamides B and C (4 pages). This material is contained in libraries on microfiche, immediately follows this article in the microfilm version of the journal, and can be ordered from the ACS; see any current masthead page for ordering information.

JO942055N